Dynamics of Nonlinear and Dispersion Managed Solitons

Qudsia Quraishi,[1,*] Steven T. Cundiff,[2] Boaz Ilan,[3] and Mark J. Ablowitz[3]

[1]*Department of Physics, University of Colorado, National Institute of Standards and Technology, and JILA, Boulder, Colorado 80309-0440, USA*

[2]*JILA, National Institute of Standards and Technology, and the University of Colorado, Boulder, Colorado 80309-0440, USA*

[3]*Department of Applied Mathematics, University of Colorado, Boulder, Colorado 80309-0526, USA*

(Received 28 February 2005; published 23 June 2005)

The relation between the fundamental parameters of energy and temporal duration of ultrashort pulses, under the condition of varying the average dispersion, are demonstrated both theoretically and experimentally in a solid-state femtosecond mode-locked laser. An asymptotic theory for nonlinear and dispersion managed solitons agrees well with the experimental data and demonstrates that the dominant factor in the pulse dynamics arises from the equilibrium established between the nonlinear Kerr effect and linear dispersion.

DOI: 10.1103/PhysRevLett.94.243904 PACS numbers: 42.65.Tg, 42.60.Fc, 42.65.Re, 42.65.Sf

Solitons are fascinating nonlinear phenomena that arise widely in physics. Solitons have a finite, localized energy and propagate unchanged. They form from the competition between linear dispersion and the nonlinear index of refraction. Surprisingly, when the sign of the linear dispersion periodically varies, as in long distance fiber communications, a new breed of soliton forms. The change in the sign of the dispersion causes these so-called dispersion managed (DM) solitons to temporally broaden and recompress or ''breathe'' as they propagate [1]. The prevalence of DM solitons has generated significant research toward understanding their behavior [2–5].

To experimentally characterize the propagation dynamics of DM solitons, a medium amenable to systematic changes in the linear dispersion is required. Such characterization has proven difficult partly because of the complexity in systematically varying the linear dispersion. The ultrashort optical pulses propagating in solid-state mode-locked lasers are also dispersion managed. However, the method by which these pulses are dispersion managed allows for systematic control over the cavity dispersion and thus, provides a near ideal environment to undertake such studies. In addition, these pulses experience a periodicity in the nonlinear refractive index, known as nonlinear management. Recent theoretical work in understanding their dynamics has shown novel behavior that is distinct from that of classical solitons [4]. Here, we report the first experimental demonstration of the systematic varying of the group velocity dispersion for a nonlinear and dispersion managed soliton. We show remarkable agreement between experiments and the DM theory of solitons for the scaling of the fundamental pulse properties of energy and temporal duration for the ultrashort pulses in a mode-locked laser. This study advances the understanding of the dynamics of the DM system in ultrashort pulsed mode-locked lasers, which have numerous important applications that rely upon pulse stability [6–10].

In the classical theory of solitons, the nonlinear Schrödinger equation (NLS) governing the pulse envelope $u(z, t)$ in an optical fiber is

$$iu_z(z, t) - \frac{\beta''}{2} u_{tt}(z, t) + \gamma_0 |u(z, t)|^2 u(z, t) = 0, \qquad (1)$$

where β'' is the group velocity dispersion (GVD) coefficient, t is the retarded time (with respect to the group delay), and $\gamma_0 = n_2\omega/cA_{\text{eff}}$ is the nonlinear coefficient for an effective transverse area A_{eff} of the beam, with center frequency ω, propagating in the z direction through a medium with a Kerr nonlinear refractive index n_2, where c is the speed of light [11]. The soliton solution for constant anomalous dispersion, $\beta'' < 0$, is $u(z, t) = A\text{sech}\,(\frac{c_0 t}{\tau}) e^{i\gamma_0 |A|^2 z/2}$, where $c_0 = 2\text{sech}^{-1}\,(1/\sqrt{2})$, A is the real-valued amplitude, and τ is the temporal FWHM. The intensity is $|A|^2 = P/A_{\text{eff}}$, where $P = E/\tau$ is the pulse power with energy $E = \int |u|^2 dt$. For the theory of classical solitons (CS), the relation between these fundamental parameters is

$$\tau = \frac{2c_0|\beta''|}{\gamma_0 E}. \qquad (2)$$

This scaling for classical solitons was observed in optical fibers [12]. No such relation has been experimentally demonstrated for DM solitons.

In the nonlinear and dispersion managed theory, $u(z, t)$ satisfies Eq. (1) with periodically varying GVD and nonlinear coefficients. Using a dispersion managed model, it was shown that stable pulses can form in a mode-locked laser [4]. A mode-locked laser is a pulsed laser that emits a periodic sequence of optical pulses where the pulses are spaced by the cavity round-trip time (the group delay, τ_g). Figure 1(a) is a schematic of a 92.8 MHz repetition-rate Kerr-lens mode-locked (KLM) Ti:sapphire laser pumped by a solid-state frequency-doubled Nd:YVO_4 laser.

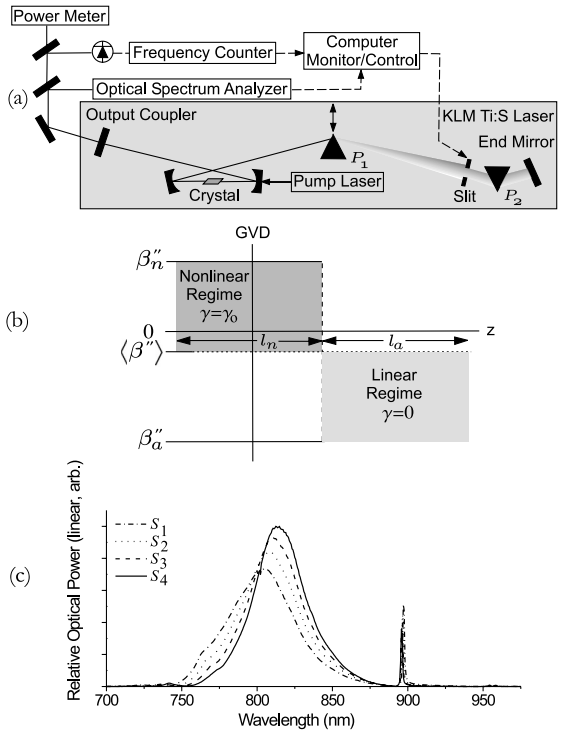

FIG. 1. (a) Schematic of a mode-locked Ti:sapphire laser, with the measurement setup. The position of the slit near prism P_2 is computer controlled to set the center frequency of mode-locked operation. (b) Schematic of the nonlinear normal GVD propagation due to the Kerr nonlinearity in the crystal and linear anomalous GVD propagation in the prism sequence. (c) Spectral profiles at four positions of the prism P_1 resulting in four different GDD values. The dash-dotted line S_1 corresponds to the most prism insertion. The spectrum narrowed as the prism was pulled out of the beam. The solid line S_4 corresponds to the least prism insertion. The sharp feature at 900 nm may be the result of the cavity mirror reflectivity characteristics.

Since such a laser can generate ultrashort pulses ($\lesssim$20 fs), the average dispersion in the cavity must be relatively small to sustain this pulse [13]. In one cavity round-trip, the pulse propagates through cavity elements with different signs of dispersion. The most significant contributions to the linear dispersion come from the normal dispersion β_n'' in the region of length l_n in the Ti:sapphire crystal, and the *compensating* anomalous dispersion β_a'' in region of length l_a in the prism sequence. For sustained, stable mode locking, the intensity of the pulse at the crystal center, after it has experienced this linear dispersion compensation, is now sufficiently high for the nonlinear Kerr effects (self- focusing and self-phase modulation) to occur so that the mode-locked operation is preferred over the continuous wave operation. For such a dispersion map the GVD, averaged over one round-trip in the cavity, $\langle\beta''\rangle$, is used to define the round-trip group delay dispersion (GDD); that is, $\langle\beta''\rangle l_t = \beta_n'' l_n + \beta_a'' l_a$, where $l_t = l_n + l_a$ is the total optical length of the cavity, as seen in Fig. 1(b). Indeed, by this definition of the round-trip GDD, the two shaded regions in Fig. 1(b) are of equal area. All other cavity elements, including air and the cavity mirrors, irrespective of their sign of GDD, only contribute to the net linear dispersion compensation provided by the cavity prism sequence and so, for simplicity, we take $l_a = l_n$.

To model this dispersion map, β'' in Eq. (1) is replaced by the local GVD, $\beta''(z)$. It is convenient to introduce the GDD variance of the dispersion map. This variance is known as the map strength s where $s = |\beta_i'' l_i - \frac{1}{2}\langle\beta''\rangle l_t|$, which is independent of the replacement of i with n or a. In the DM theory, s arises naturally as a physically relevant and theoretically important parameter [14,15]. The *reduced* map strength $M = s/(\langle\beta''\rangle l_t)$ is the relative strength of the GDD variance with respect to the round-trip GDD. The nonlinearity must also be managed in the theory, with the replacement $\gamma = \gamma_0$ in the crystal and $\gamma = 0$ elsewhere, so now $\gamma = \gamma(z)$. This nonlinear and dispersion managed equation is referred to as the perturbed NLS (PNLS),

$$iu_z(z,t) - \frac{\beta''(z)}{2}u_{tt}(z,t) + \gamma(z)|u(z,t)|^2 u(z,t) = 0. \quad (3)$$

Figure 1(b) shows the nonlinear and dispersion maps of the laser in one cavity round-trip. For the DM theory, three experimental input parameters, $\langle\beta''\rangle l_t$, γ_0, and s, are required to model the fundamental propagation dynamics.

To characterize the experimental relation between the fundamental pulse properties, we recorded E as a function of τ for various values of the average cavity GDD, $\langle\beta''\rangle l_t$. In the mode-locked laser, dispersion causes the group delay of the pulse ($\tau_g = 1/f_{\text{rep}}$, where f_{rep} is the repetition rate) to depend upon the center frequency ω of the mode-locked spectrum. Actively controlling the center frequency through the use of a slit in the cavity, positioned after the prism P_1, permits one to map $\tau_g(\omega)$ and thus, to measure the round-trip GDD [Fig. 1(a)] [16]. For a given prism P_1 insertion, the slit near P_2 was situated in the cavity beam with the slit opening adjusted to reduce the bandwidth while still permitting mode locking. The slit was then translated transversely to the beam and at each slit position the spectrum was recorded with an optical spectrum analyzer and f_{rep} was measured by an RF frequency counter. The center frequency was calculated from the first moment of the recorded optical spectrum. The GDD is given by the linear coefficient of a least-squares fit to these data. From this measured value of the GDD, the anomalous GDD of the prism sequence and s are calculated. Since the nonlinearity occurs in a small region (within the Rayleigh range of the beam focus) in the Ti:sapphire crystal (length of 2.3 mm), we set $l_n = 0.5$ mm so $\beta_n'' l_n = +30$ fs^2($\beta_n'' = +60$ fs^2/mm). To minimize the cavity GDD for more stable mode locking, we use dispersion compensated mirrors (DCM) [17]. Since the prism sequence (and DCMs) provide dispersion compensation up to second order, higher order contributions are minimized by using prisms

made of CaF_2. Drift of the repetition rate arising from cavity length fluctuations can disturb or even prohibit the measurement of the GDD. This drift has been observed to vary linearly with time and was minimized by isolating the laser in a plexiglass enclosure. Additionally, the data acquisition was automated so that the GDD was measured in less than 60 sec and corrected for the drift.

To systematically change the cavity GDD, the first prism P_1 was successively translated into the beam [Fig. 1(a)]. The (fixed) separation between the prisms determines the amount of anomalous compensation, while each prism's individual differential insertion into the beam determines the added normal dispersion [Fig. 1(c)]. For each GDD setting, the pump laser power was used to control the intracavity pulse energy E and was ramped through the full stability range of mode locking.

To gain insight into the fundamental governing dynamics, an asymptotic analysis may be undertaken. The quantity l_n/l_0, where $l_0 = 1/(\gamma_0 P)$, is a measure of the length over which the nonlinearity causes a 2π-phase shift in the pulse. A perturbative expansion of the PNLS [Eq. (3)] to first order in l_n/l_0 yields the dispersion managed nonlinear Schrödinger equation (DMNLS)

$$i\hat{U}_z(z,\omega) + \frac{\langle\beta''\rangle}{2}\omega^2\hat{U}(z,\omega) + \frac{\gamma_0}{2}\iint_{-\infty}^{+\infty}\frac{\sin(\omega_1\omega_2 s)}{\omega_1\omega_2 s} \times \hat{U}(z,\omega+\omega_1)\hat{U}(z,\omega+\omega_2) \times \hat{U}^*(z,\omega+\omega_1+\omega_2)d\omega_1 d\omega_2 = 0. \quad (4)$$

The nonlinear management yields the factor of $1/2$ in the nonlocal term and so doubles the pulse energy as compared to the usual DM solitons with a constant nonlinear coefficient. The DMNLS is a nonlocal equation and admits localized stable solutions known as DM solitons,

$$\hat{U}(z,\omega) = e^{i(\lambda^2/2)z}\hat{f}(\omega), \quad (5)$$

where λ^2 is a constant and $\hat{f}(\omega)$ is real and symmetric [14]. When these solutions seed the PNLS, they remain localized and stable while acquiring an additional phase term. This frequency dependent phase introduces a chirp in the pulse, with a period related to the periodicity of the dispersion map. As the DM soliton propagates from the center of the normal region, it temporally broadens and then recompresses until it reaches the center of the anomalous region, whereupon it begins to broaden again, thereby breathing, as seen in the inset in Fig. 2, whereas the classical soliton does not breathe. The full (PNLS) solution, written in terms of the DM soliton is

$$u(z,t) = \mathcal{F}^{-1}[\hat{U}(z,\omega)e^{-i(\omega^2/2)\int_0^z[\beta_i''(z)-\langle\beta''\rangle]}]. \quad (6)$$

The DMNLS, unlike the PNLS, has constant coefficients. Another significant advantage of the DMNLS is that the rapidly varying phase associated with the breathing is removed and the DM soliton solution is readily obtained.

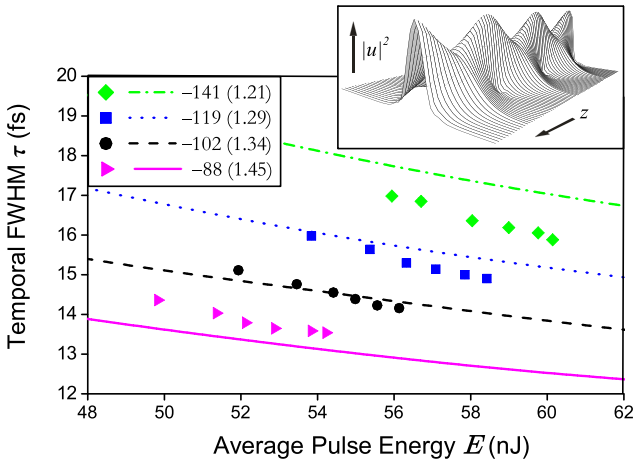

FIG. 2 (color online). Scaling of the fundamental pulse parameters in a mode-locked Ti:sapphire laser. The points are the measured temporal FWHM at the four values of the average cavity GDD. The curves are the solutions of Eq. (4), where one data point (54.4 nJ, 14.6 fs) was used to fit γ_0. The legend states both the GDD values in fs^2 (and the corresponding M values). The errors for the GDD are approximately 1% and the errors for the τ values are negligible on the scale shown. The spectra in Fig. 1(c) correspond to each of the highest E values (S_1 corresponds to the point at 54.2 nJ). The inset shows the breathing dynamics of a dispersion managed soliton $|u|^2$ [Eq. (6)] propagating along z.

Thus, the energy E and the temporal FWHM τ are calculated from Eq. (5).

The experimental data for the temporal FWHM dependence upon the intracavity pulse energy for four values of the GDD are plotted in Fig. 2. Since the theoretical model predicts the pulse duration at the crystal center ($z = 0$), the width τ for each E setting was determined assuming a transform-limited optical spectrum. In this regime, as the GDD becomes more anomalous, the pulse requires higher energies to remain stably mode locked. The theoretical curves are plotted in Fig. 2 where each is distinguished by the value of the reduced map strength, M. Given that the mechanisms for mode locking are not included in the model, the curves show remarkable agreement with the data and accurately predict the pulse dynamics over a broad range of parameters.

In generating the theoretical nonlinear and dispersion managed solutions, only one fitting parameter is used. The experimental uncertainty in the effective area A_{eff} of the beam at the center of the crystal requires that the nonlinear coefficient γ_0 be fit to match the data ($n_2 = 3.2 \times 10^{-8}$ mm^2/MW). Fitting one experimental data point, we find $A_{\text{eff}} = 200$ μm^2 and so $\gamma_0 = 1.26(mm \cdot MW)^{-1}$. Since our model uses only one fitting parameter, here we have explicitly determined γ_0 for an ultrashort pulsed mode-locked laser.

The formation of a mode-locked pulse in a Ti:sapphire laser requires gain and loss mechanisms that have so far

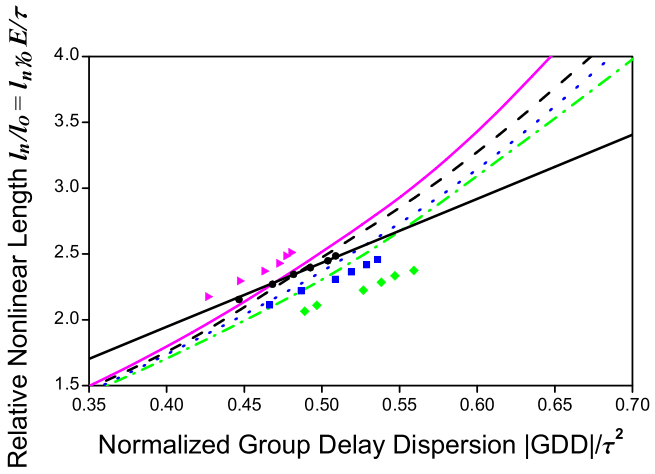

FIG. 3 (color online). Plot of the scaling of the asymptotic parameter with the normalized GDD, where the reduced map strength M is fixed for each of the theoretical curves. The solid line corresponds to the CS theory using Eq. (2) where one data point was used to fit γ_0. The curves are from the nonlinear and dispersion managed theory [Eq. (4)] and correspond to the same M values (with their respective colors and line types) as those given in Fig. 2. The experimental data are those from Fig. 2, with the appropriate scaling each pair of E and GDD with τ.

been neglected in the model. Such effects typically include saturable absorption, saturable gain, and spectral filtering and, when included in the theoretical model, the governing equation is called the master equation for mode locking [18]. We have included saturable absorption and gain in the theoretical model (in the PNLS) and have confirmed that the predictions are largely insensitive to these processes. Consequently, this simplifies the theory for the understanding of the propagation of pulses in mode-locked lasers, establishing that though these gain and loss processes are necessary to generate the pulse, the pulse's subsequent dynamics is well governed by the DM theory [Eq. (4)]. Hence, the pulse's behavior is dominated by the competing mechanisms of the Kerr nonlinearity and linear dispersion.

For the CS theory ($s = 0$) there is a fixed relationship between l_n/l_0 and the normalized GDD, $|\langle\beta''\rangle|l_t/\tau^2$, as seen in Eq. (2). In the DM theory, the additional parameter of s changes this relation and predicts the separation between the curves observed experimentally, as seen in Fig. 3. The CS line was obtained by fitting γ_0 in Eq. (2) to one data point. As the energy E vanishes, the soliton is not sustained, and hence, the DM (and CS) curves converge to zero (not shown). We also note that the Ti:sapphire laser is in a regime where l_n/l_0 is $\mathcal{O}(1)$. Nevertheless, our asymptotic theory for this regime still agrees with the direct numerical simulations to the PNLS equation.

In summary, for the solitons propagating in mode-locked Ti:sapphire lasers, the agreement between the PNLS and the experimental data demonstrates that the dominant factor in the pulse dynamics is the equilibrium established between the Kerr nonlinearity and the linear dispersion. We have used an asymptotic theory developed for the PNLS to predict the dynamics of these solitons using only one fitting parameter in the model to generate the theoretical curves. This study shows that the dispersion management concepts originally developed in fiber communications apply in a much broader context.

This research was partially supported by the U.S. Air Force Office of Scientific Research under Grant No. 1-49620-03-1-0250. The work at JILA was supported by the NSF, NIST, and the University of Colorado, Department of Physics.

*Electronic address: quraishi@colorado.edu

[1] C. Lin, H. Kogelnik, and L. G. Cohen, Opt. Lett. **5**, 476 (1980).
[2] F. O. Ilday, J. R. Buckley, W. G. Clark, and F. W. Wise, Phys. Rev. Lett. **92**, 213902 (2004).
[3] M. Suzuki and N. Edagawa, J. Lightwave Technol. **21**, 916 (2003).
[4] Y. Chen, F. X. Kärtner, U. Morgner, S. H. Cho, H. A. Haus, E. P. Ippen, and J. G. Fujimoto, J. Opt. Soc. Am. B **16**, 1999 (1999).
[5] N. Smith, F. Knox, N. Doran, K. Blow, and I. Bennion, Electron. Lett. **32**, 54 (1996).
[6] D. Meshulach and Y. Silberberg, Nature (London) **396**, 239 (1998).
[7] S. A. Diddams *et al.*, Science **293**, 825 (2001).
[8] Th. Udem, R. Holzwarth, and T. W. Hänsch, Nature (London) **416**, 233 (2002).
[9] *Femtosecond Optical Frequency Comb Technology*, edited by J. Ye and S. T. Cundiff (Springer, New York, 2004).
[10] *Ultrafast Phenomena XIV*, edited by T. Kobayashi, T. Okada, T. Kobayashi, K. A. Nelson, and S. De Silvestri (Springer, New York, 2004), Vol. 79.
[11] A. Hasegawa and F. D. Tappert, Appl. Phys. Lett. **23**, 142 (1973).
[12] L. F. Mollenauer and R. H. Stolen, Opt. Lett. **9**, 13 (1984).
[13] M. T. Asaki, C. P. Huang, D. Garvey, J. Zhou, H. C. Kapteyn, and M. M. Murnane, Opt. Lett. **18**, 977 (1998).
[14] M. J. Ablowitz and G. Biondini, Opt. Lett. **23**, 1668 (1998).
[15] M. J. Ablowitz, B. Ilan, and S. T. Cundiff, Opt. Lett. **29**, 1808 (2004).
[16] W. H. Knox and J. P. Gordon, J. Opt. Soc. Am. B **10**, 2071 (1993).
[17] G. Tempea, F. Krausz, C. Spielmann, and K. Ferencz, IEEE J. Sel. Top. Quantum Electron. **4**, 193 (1998).
[18] H. Haus, IEEE J. Sel. Top. Quantum Electron. **6**, 1173 (2000).